






# Extruded tellurite antiresonant hollow core fiber for Mid-IR operation

ANDREA VENTURA,<sup>1,\*</sup> JULIANO GRIGOLETO HAYASHI,<sup>1</sup> JAROSLAW CIMEK,<sup>1</sup> GREGORY JASION,<sup>1</sup>  PETR JANICEK,<sup>2,3</sup> FEDIA BEN SLIMEN,<sup>1</sup> NICHOLAS WHITE,<sup>1</sup> QIANG FU,<sup>1</sup>  LIN XU,<sup>1</sup> HESHAM SAKR,<sup>1</sup>  NATALIE V. WHEELER,<sup>1</sup> DAVID J. RICHARDSON,<sup>1</sup> AND FRANCESCO POLETTI<sup>1</sup>

<sup>1</sup>Optoelectronics Research Centre, University of Southampton, Southampton SO17 1BJ, UK

<sup>2</sup>Institute of Applied Physics and Mathematics, Faculty of Chemical Technology, University of Pardubice, Pardubice 53210, Czech Republic

<sup>3</sup>Center of Materials and Nanotechnologies, Faculty of Chemical Technology, University of Pardubice, Pardubice 53210, Czech Republic

\*av1d16@soton.ac.uk

**Abstract:** We report the first extruded tellurite antiresonant hollow core fibers (HC-ARFs) aimed at the delivery of mid-infrared (Mid-IR) laser radiation. The preform extrusion fabrication process allowed us to obtain preforms with non-touching capillaries in a single step, hence minimizing thermal cycles. The fibers were fabricated from in-house synthesized tellurite glass (containing Zn, Ba and K oxides) and co-drawn with a fluorinated ethylene propylene (FEP) polymer outer layer to improve their mechanical properties and protect the glass from humidity. The fabricated HC-ARFs transmit in the Mid-IR spectral range from 4.9 to 6  $\mu\text{m}$ . We measured losses of  $\sim$ 8.2, 4.8 and 6.4 dB/m at 5  $\mu\text{m}$ , 5.6  $\mu\text{m}$  and 5.8  $\mu\text{m}$ , respectively in two different fibers. These losses, which are dominated by leakage mostly arising from a non-uniform membrane thickness, represent the lowest attenuation reported for a tellurite-based HC-ARF to date. The fibers present good beam quality and an  $M^2$  factor of 1.2. Modelling suggests that by improving the uniformity in the capillary membrane thickness losses down to 0.05 dB/m at 5.4  $\mu\text{m}$  should be possible, making this solution attractive, for example, for beam delivery from a CO laser.

Published by The Optical Society under the terms of the [Creative Commons Attribution 4.0 License](https://creativecommons.org/licenses/by/4.0/). Further distribution of this work must maintain attribution to the author(s) and the published article's title, journal citation, and DOI.

## 1. Introduction

Medical, industrial and military applications, such as surgery, material cutting and welding, rely on mid-infrared (Mid-IR) laser delivery [1,2]. Various types of solid core optical fibers for Mid-IR laser delivery have been developed in the past, but, as in these fibers light is guided in the glass material, they all tend to suffer from limitations imposed by the Mid-IR glass. For example, chalcogenide-based solid core fibers have low laser induced damage threshold and high non-linearity and they are therefore not suitable for high power beam delivery applications [3,4]. Hollow core microstructured optical fibers (HC-MOFs) offer an alternative; in these fibers, >99.9% of the guided light propagates in air, which provides a route to overcome these limitations. Hollow core antiresonant fibers (HC-ARFs) are a specific type of HC-MOF which have an extremely low overlap of the guided mode with the cladding glass, down to  $5 \times 10^{-5}$  for specific designs [5]. Such a low glass overlap opens up a host of interesting fiber properties, including low non-linearity, high damage threshold and the potential for ultra-low loss [5] and for light transmission at wavelengths beyond the transmission window of a given material. In addition, HC-ARFs can be designed to be effectively single mode despite a large core size [5]. It has been

shown that HC-ARFs with non-touching capillaries offer lower transmission loss than HC-ARFs with touching capillaries and hence glass nodes [6]. Whilst silica is the material of choice for near IR applications for its excellent transmission, silica HC-ARFs can provide guidance with practically low optical loss up to  $\sim 4.5 \mu\text{m}$  [6,7]. For longer wavelengths, soft-glasses such as tellurite and chalcogenide glasses represent a solution to extend the transmission up to  $\sim 6.5$  and  $\sim 12 \mu\text{m}$ , respectively.

To date, several tubular HC-ARFs, consisting of cladding tubes inside a jacket tube, designed for Mid-IR laser delivery have been developed. Kosolapov et al. [8] reported a HC-ARF made from  $\text{Te}_{20}\text{As}_{30}\text{Se}_{50}$  chalcogenide glass with 8 touching capillaries by using the stack and draw technique. The fiber had an outer diameter (OD) of  $750 \mu\text{m}$ , a core diameter of  $380 \mu\text{m}$  and a capillary thickness of  $13 \mu\text{m}$ . Some of the capillaries were detached from the jacket of the fiber (capillary dislocation). The measured optical loss was  $11 \text{ dB/m}$  at  $10.6 \mu\text{m}$ . Shiryaev et al. [9] reported a HC-ARF with 8 touching capillaries made of  $\text{As}_2\text{S}_3$  chalcogenide glass also using the stack and draw approach. During the draw, some of the capillaries were also dislocated. The applied gas pressure into the capillaries was changed until a symmetric structure was obtained. The fiber loss was  $3 \text{ dB/m}$  at  $4.8 \mu\text{m}$ . Gattass et al. [10] developed a tubular antiresonant preform by extruding a billet of  $\text{As}_2\text{S}_3$  chalcogenide glass. The extruded preform was then drawn into a fiber without capillary dislocations. The fiber had a core diameter of  $\sim 172 \mu\text{m}$  and a capillary thickness of  $7 \mu\text{m}$ . The measured loss was  $2$  and  $2.1 \text{ dB/m}$  at the wavelengths of  $5$  and  $10 \mu\text{m}$ , respectively. Belardi et al. [11] fabricated a borosilicate HC-ARF with non-touching tubes. The fiber had a core of  $122 \mu\text{m}$  diameter and an outer diameter of  $400 \mu\text{m}$ . The fiber loss was  $4 \text{ dB/m}$  for wavelengths between  $5$  and  $5.2 \mu\text{m}$ . Tong et al. [12] fabricated a tellurite HC-ARF by stacking 6 non-touching capillaries. The capillaries thickness was  $2.8 \mu\text{m}$ . They measured the transmission through a  $17 \text{ cm}$  long fiber for wavelengths between  $2$  and  $3.9 \mu\text{m}$  but without determining the transmission loss.

In this work, we present the first, to the best of our knowledge, tellurite HC-ARFs for laser delivery in the Mid-IR, fabricated through the extrusion and draw method. The tellurite HC-ARFs were co-drawn with a fluorinated ethylene propylene (FEP) polymer. Tellurite glass is non-toxic compared to some of the chalcogenide glasses and, according to our numerical modelling, could allow for an optical loss lower than  $1 \text{ dB/m}$  up to  $6.5 \mu\text{m}$  wavelength. We demonstrate Mid-IR transmission through our tellurite HC-ARFs with losses of  $8.2 \pm 0.6 \text{ dB/m}$ ,  $4.8 \pm 0.4 \text{ dB/m}$  and  $6.4 \pm 0.4 \text{ dB/m}$  at  $5$ ,  $5.6$  and  $5.8 \mu\text{m}$ , respectively. The beam quality of light transmitted through  $13 \text{ cm}$  of a fabricated tellurite HC-ARF was also measured and an  $M^2$  factor of  $1.2$  was obtained, confirming that our fabricated HC-ARF supports a good beam quality and is effectively single-mode since the high order modes have high losses compared to the fundamental mode. The FEP polymer coating gives the fabricated fibers strength, flexibility and protection from the environment. This represents a big practical advantage compared to the mostly uncoated fibers reported in the literature (which are generally very fragile as a result) [8–10,12]. The tellurite HC-ARFs reported here are durable, protected from moisture, and can be bent with a curvature radius of  $4 \text{ cm}$  without breaking.

## 2. Characterization of the tellurite glass

The material used for the reported HC-ARFs was tellurite glass. The glass composition of  $70\text{TeO}_2\text{-}13\text{ZnO-}10\text{BaO-}7\text{K}_2\text{O}$  developed by Zhou et al. [13] was synthesized-in-house. This glass was chosen because of its long cut-off wavelength ( $6.1 \mu\text{m}$ ) and its high thermal stability. In comparison to other mid-infrared glasses like chalcogenide and fluoride, tellurite glasses can be easily modified by changing their chemical composition. Furthermore, while fluoride glasses have great transmission in the mid-infrared and low nonlinearity, their thermal stability is low and their synthesis is difficult [14]. Also the chemical durability of fluoride glasses and some chalcogenide glasses is very low [15,16]. Tellurite glasses can be synthesized in large

volumes and do not require a protective atmosphere as opposed to fluoride and chalcogenide glass fabrication. Moreover, tellurite glasses are not toxic (unlike chalcogenide glasses) and have better crystallization resistance than fluoride glasses which is critical for fiber drawing [17]. The tellurite glass used in current work was melted in a gold crucible at 800°C for 2 hours. A calorimetric measurement was performed on a powdered glass sample by using a PerkinElmer Diamond Thermogravimetry/ Differential Thermal Analysis (TG/DTA), as shown in Fig. 1. The glass transition temperature ( $T_g$ ) is 297.6 °C. In the TG/DTA curve in Fig. 1, the lack of a crystallization peak above the  $T_g$ , confirms the high thermal stability of the glass.

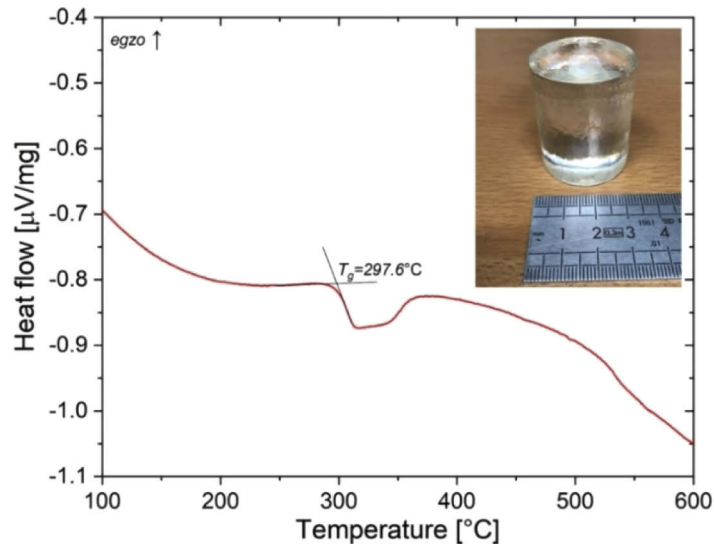


**Fig. 1.** TG/DTA curve of the fabricated tellurite glass. The inset shows a made-in-house tellurite glass billet.

The refractive index of the glass, shown in Fig. 2(a), was measured on a polished glass sample using a variable angle spectroscopic ellipsometer IR-VASE (J.A. Woollam Co.) which covers the wavenumber spectral range of  $840\text{ cm}^{-1}$  -  $5500\text{ cm}^{-1}$  (NIR-MIR). Spectra for angles of incidence (AOI) of  $55^\circ$ ,  $60^\circ$ ,  $65^\circ$  and  $70^\circ$  were recorded (measuring 25 scans, 15 spectra per revolution, with wavenumber step was  $8\text{ cm}^{-1}$ ). The back of the sample was roughened to avoid undesirable reflection from this facet.

For accurate glass attenuation, the internal transmission was determined using Varian 670-IR spectrometer. The absorbance spectra of two samples with different thicknesses (3 mm and 15 mm) were measured. The difference between the absorbance spectra was then normalized to represent a 10 mm thick sample. From that, the internal transmission without Fresnel loss was calculated [blue curve in Fig. 2(b)]. The normalization was performed in order to compare our tellurite glass transmission with the transmission spectrum of a 10 mm thick sample of fused silica glass which was extracted from Ref. [18] [Fig. 2(b)]. As seen in Fig. 2(b), the glass synthesized in-house transmits significantly better than silica from 3.5 to 6.1  $\mu\text{m}$ . It is therefore to be expected that tellurite HC-ARFs should transmit well beyond the longest transmission wavelength achieved in silica HC-ARFs (4.5  $\mu\text{m}$ ).

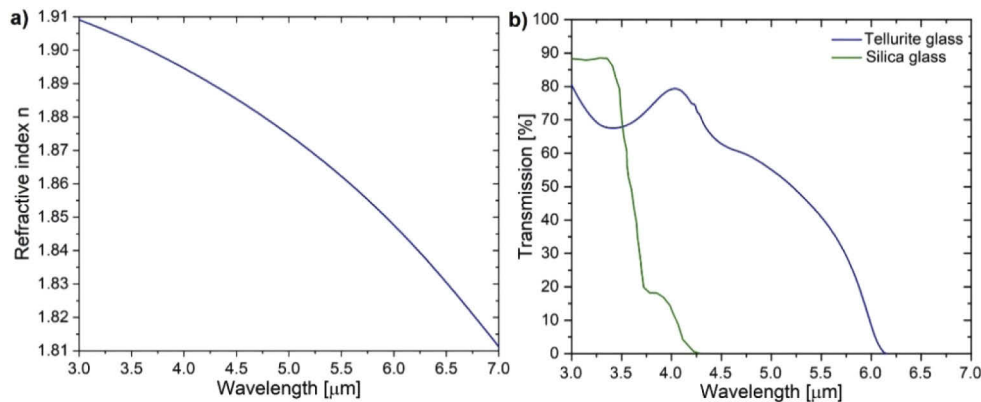


**Fig. 2.** (a) Tellurite glass refractive index measured using a variable angle spectroscopic ellipsometer IR-VASE, J.A. Woollam Co. (b) Transmission spectrum of fabricated tellurite glass normalized on a sample 10 mm thick (blue curve) and transmission spectrum of silica glass for a sample 10 mm thick (green curve) (Reproduced from Heraeus [18]).

### 3. Antiresonant hollow core fiber fabrication

The tellurite HC-ARF in this work was designed to have low loss in the wavelength range between 5 and 6 μm, which is compatible, for example, with the delivery of CO laser radiation at 5.4 μm, and useful for material cutting, welding and surgery [1,2]. Fabricating a fiber operating in the fundamental or in the second transmission band, would require capillaries with thicknesses smaller than 3 μm, which is challenging at present. For this reason, we have decided to target operation in the third transmission band, which represents a good trade-off between the capillary thickness which can be achieved in the fiber draw and the spectral width of transmission band, which is reduced but still adequately wide. Simulations suggested that the minimum loss at 5.4 μm could be achieved for a capillaries thickness of 4.4 μm. In particular, the target fiber had a core diameter of 125 μm and 6 non-touching and perfectly circular capillaries with an inner diameter of 73 μm. Simulations on such a perfectly symmetric tellurite fiber structure show a predicted loss as low as 0.05 dB/m at 5.4 μm.

Overall, from the work reported in the literature and discussed above in the introduction, two techniques have been used to develop HC-ARFs made of soft-glasses. These are the stack and draw and the extrusion and draw approaches. While stack and draw techniques are popular for fabricating silica microstructured fibers, in part due to the commercial availability of high precision tubes, the fabrication of symmetric fibers by stack and draw with soft-glasses is more difficult. This is due to their lower mechanical strength, steeper viscosity-temperature curves and propensity to crystallization in processes requiring multiple re-heatings [17]. To overcome these difficulties, in this work, we chose the extrusion and draw approach to fabricate tellurite HC-ARFs. The main advantage of this technique is that it allows for preforms with non-touching capillaries that are well fused to the jacket glass tube, which avoids capillary dislocation during the fiber drawing. Capillary dislocation which causes non-uniformity in the fiber, can lead to an inadequately low beam quality and high confinement loss [8]. In addition, it is difficult to stack tellurite glass capillaries due to their fragility. Moreover, since the consolidation step of the stack and draw approach is not needed, the extrusion process minimizes the thermal steps required to fabricate the preform.

For this work, the stainless steel extrusion die shown in Fig. 3(a) was designed with an outer diameter (OD) of 13 mm, and with 6 non-touching circular tubes of 3.68 mm OD and 250 μm thickness. An in-house-made tellurite glass billet of 32 mm OD and 36 mm in length (shown in

the inset of Fig. 1) was extruded at 340 °C. The cross-section of the extruded preform is shown in Fig. 3(b). As shown in Fig. 3(c), 20 cm of the extruded preform were straight and free of any defect or sign of crystallization. The inner diameter (ID) and OD of the preform were 11.08 and 13.3 mm, respectively. The capillary thickness was  $228 \pm 13 \mu\text{m}$ . As can be seen, due to surface tension effects, the capillaries are not completely circular and the preform has acquired a hexagonal shape.

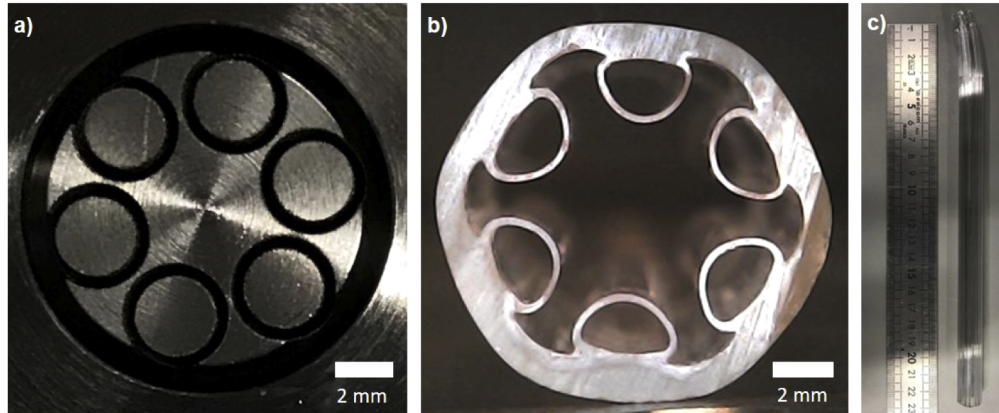


**Fig. 3.** (a) Extrusion die, (b) cross-section and (c) side of the tellurite glass extruded preform.

In previous work reported in the literature [8–10,12], no coating was applied to the tellurite or chalcogenide HC-ARFs. The absence of a coating in these glass fibers can have a profound effect on their ultimate mechanical strength and flexibility, and leads to fiber deterioration with time due to reaction of the glass with moisture [16]. To overcome these problems, in this work, a FEP polymer was chosen as a protective jacket for the HC-ARF. Its low Young's modulus (600 MPa) [19] makes the fiber flexible and mechanically strong. This polymer, which has a processing temperature of 370 °C [20], is thermally compatible with the tellurite glass. The preform was inserted in a FEP polymer tube with 15 mm ID and 17 mm OD, and the preform and FEP polymer tube were co-drawn into a fiber at 350 °C. During the draw, the capillaries were selectively pressurized with argon to counterbalance the effect of surface tension. This is important to achieve the desired capillaries thickness and control the core dimension and inter-capillary gap. The core was left at atmospheric pressure. The fiber drawing was started with no pressure applied into the capillaries and then the pressure was increased during the draw in order to get a fiber structure close to the target fiber. Figure 4(a) shows a scanning electron microscope (SEM) picture of a tellurite HC-ARF fabricated by applying 6 mbar of pressure into the capillaries (Fiber A). The fiber, 9 meters long, has an OD  $\sim 400 \mu\text{m}$ , a core diameter of  $187 \mu\text{m}$  and an average capillary thickness of  $5.7 \mu\text{m}$  with a standard deviation of  $0.3 \mu\text{m}$ . The fiber shown in Fig. 4(b), was fabricated from another preform extruded at the same conditions of the one in Fig. 3(b), by applying 5.2 mbar of pressure into the capillaries (Fiber B). The fiber is 9 meters long, has an OD  $\sim 300 \mu\text{m}$ , a core diameter of  $139 \mu\text{m}$  and an average capillary thickness of  $5 \mu\text{m}$  with a standard deviation of  $0.2 \mu\text{m}$ .

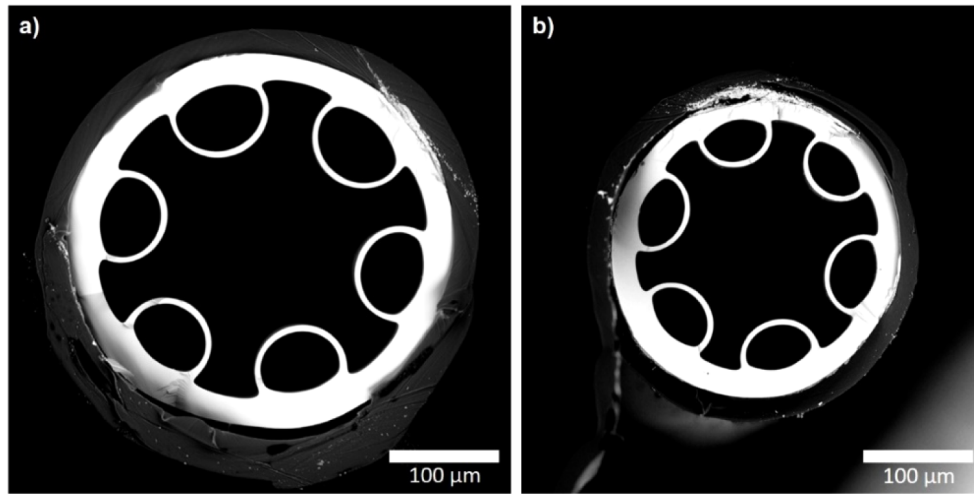


**Fig. 4.** SEM pictures of (a) the tellurite HC-ARF developed by applying 6 mbar of pressure into the capillaries (Fiber A) and (b) the tellurite HC-ARF fabricated by applying 5.2 mbar of pressure into the capillaries (Fiber B).

#### 4. Fiber characterization and modelling

The fabricated tellurite HC-ARFs have been characterized and the experimental results compared with simulations. The loss of Fiber A was measured by using an FTIR spectrometer. Infrared radiation from a Thorlabs SLS202L Stabilized Tungsten lamp was coupled into a 36 cm long fiber. The output of the fiber, as imaged using a Xenics Onca MWIR 320 thermal camera which operates between 3.6 and 4.9  $\mu\text{m}$  and shown in the inset of Fig. 5(a), indicates that most of the infrared light is transmitted in the core. The fiber transmission was measured with an ARCoptix FT-IR rocket spectrometer. A cut-back measurement was performed by measuring the transmission spectrum of the fiber 4 times (3 cuts) from 36 cm to 11.5 cm. Between 4.8 and 5.2  $\mu\text{m}$ , the Fiber A shows loss between 6.8 and 36.8 dB/m [solid light blue curve in Fig. 5(a)]. The minimum measured loss was at 5.11  $\mu\text{m}$ . In order to verify this measurement, a cut-back was also performed on an adjacent piece of fiber by using an Optical Parametric Oscillator (OPO) with good beam quality [21] at the two wavelengths of 4.9 and 5  $\mu\text{m}$ . At 4.9  $\mu\text{m}$ , the output power was measured twice with a power meter for a 1.10 m and a 0.91 m piece (1 cut). For the 5  $\mu\text{m}$  measurement we measured the output power 4 times from 91 cm to 69 cm (3 cuts). The loss measured in this way was 14.2 and  $8.2 \pm 0.6$  dB/m at 4.9 and 5  $\mu\text{m}$ , respectively [black squared dots in Fig. 5(a)]. As shown in Fig. 5(a), these values of loss match very well with the losses measured by FTIR.

To measure the loss of Fiber B, two cut-backs were performed in a similar way using the OPO tuned to both 5.6 and 5.8  $\mu\text{m}$ . At 5.6  $\mu\text{m}$  we performed 3 cuts (4 measurements) from 1.16 m to 0.9 m, while at 5.8  $\mu\text{m}$  we did 2 cuts from 0.99 to 0.7 m. The measured loss was  $4.8 \pm 0.4$  dB/m at 5.6  $\mu\text{m}$  and  $6.4 \pm 0.4$  dB/m at 5.8  $\mu\text{m}$  [black squared dot in Fig. 5(b)].

These measured losses were then compared with finite element method (FEM) simulations made using Comsol Multiphysics. The exact cross-section of the fibers was extracted from the SEM images of the fabricated fibers and imported into Comsol. The real part of the refractive index of tellurite glass shown in Fig. 2(a) was used. For the imaginary part of the refractive index of the glass the FTIR loss measurement was used up to 6.1  $\mu\text{m}$  [Fig. 2(b)], and then the ellipsometry result for longer wavelengths. The two measurements agree fairly well, although a kink can be seen in the black curve in Fig. 5(b) at the switch-over wavelength. To avoid

reflections at the external boundary of the fiber, a perfectly matched layer was used [22]. A mesh size of  $\lambda/6$  was used both in the air and in the glass regions. The final mesh was composed of  $\sim 2,000,000$  degrees of freedom (DoF). The simulated total loss (i.e. confinement plus glass absorption contribution) of the fabricated fibers is shown in Figs. 5(a) and 5(b) (solid red curves). The simulated loss of Fiber A is between 1.9 and 31.6 dB/m in the 4.8-5.4  $\mu\text{m}$  spectral range, showing the minimum loss at 4.97  $\mu\text{m}$  [solid red curve in Fig. 5(a)]. Fiber B has a simulated loss between 2.4 and 78 dB/m in the 5.4-6.5  $\mu\text{m}$  wavelength range [solid red curve in Fig. 5(b)]. To assess the origin of these losses, the confinement loss of the fiber was also simulated in isolation while setting material losses to zero (dashed black curve). The expected contribution from material absorption is inferred by subtracting the confinement loss contribution from the total loss simulation, and is shown as a green curve. As can be seen, in both fibers the material absorption loss is one to two orders of magnitude lower than the confinement contribution, which hence dominates the overall loss. This could be due to the large gaps between the capillaries and non-uniformities in the capillaries.

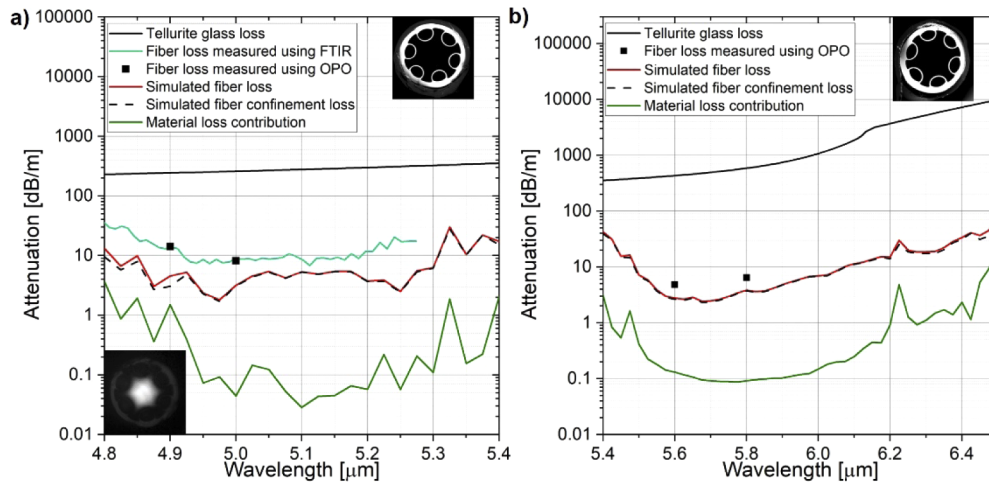


**Fig. 5.** Attenuation simulated for Fiber A (a) and Fiber B (b) (solid red curve). The dashed black curve represents the simulated confinement loss of the fabricated fiber. The light blue curve represents the fiber loss measured using the FTIR. The black squared dots represent the fiber loss measured using the OPO. The green curve represents the modelling material loss contribution. The black solid curve represents the loss of the fabricated tellurite glass. The inset of (a) shows a thermal image of the output of Fiber A when the Thorlabs tungsten lamp was coupled into a 36 cm long fiber.

Table 1 compares the measured and simulated losses of Fiber A and Fiber B. The measured losses in both fibers are somewhat higher than the simulation results. This could be attributed to a slight non-uniformity along the fiber which is not captured by a simulation of an end cross-section, and potentially by other sources of loss like scattering and microbending which were not included in the simulation.

It is also interesting to observe that despite having a larger core, which normally would be expected to decrease the straight leakage loss, Fiber A actually has a higher loss than Fiber B, and its loss is also more spectrally structured. This is observed in both measurement and simulation. This might be explained by the fact that, as a result of a small difference between the two extruded preforms, probably arising from a small change in the quality of the two extruded billets which might result in a locally changing viscosity in the two glasses, Fiber B has capillaries with a smaller thickness non-uniformity than Fiber A. The standard deviation from the average capillary

thickness measured by our image analysis software decreases from 0.3  $\mu\text{m}$  in Fiber A to 0.2  $\mu\text{m}$  in Fiber B, and this, as we will show in the next section, can have a non-negligible impact on the overall loss. In addition, Fiber A and Fiber B transmit in the 4th and 3rd transmission bands, respectively. This makes the transmission band of Fiber A narrower and more susceptible to degradation through structural imperfections, which might explain the noisier spectral loss.

**Table 1. Comparison between the measured and simulated losses of Fiber A and Fiber B.**

	OD ( $\mu\text{m}$ )	Core diameter ( $\mu\text{m}$ )	Capillary thickness ( $\mu\text{m}$ )	Loss measured using FTIR		Loss measured using OPO		Simulated loss	
				$\lambda$ ( $\mu\text{m}$ )	Loss (dB/m)	$\lambda$ ( $\mu\text{m}$ )	Loss (dB/m)	$\lambda$ ( $\mu\text{m}$ )	Loss (dB/m)
				Fiber A	400	187	$5.7 \pm 0.3$	4.9	13.8
				5.0	8.8	5.0	$8.2 \pm 0.6$	5.0	3.2
Fiber B	300	139	$5.0 \pm 0.2$	5.6	-	5.6	$4.8 \pm 0.4$	5.6	2.8
				5.8	-	5.8	$6.4 \pm 0.4$	5.8	3.8

Since hollow core fibers are sensitive to bending [23], the bend loss of Fiber B, which has the lowest measured loss, was simulated as a function of the radius of curvature. The refractive index of the glass was modified according to the standard conformal transformation [24]. Figure 6(a) shows the bending loss simulation of Fiber B at 5.6  $\mu\text{m}$ .

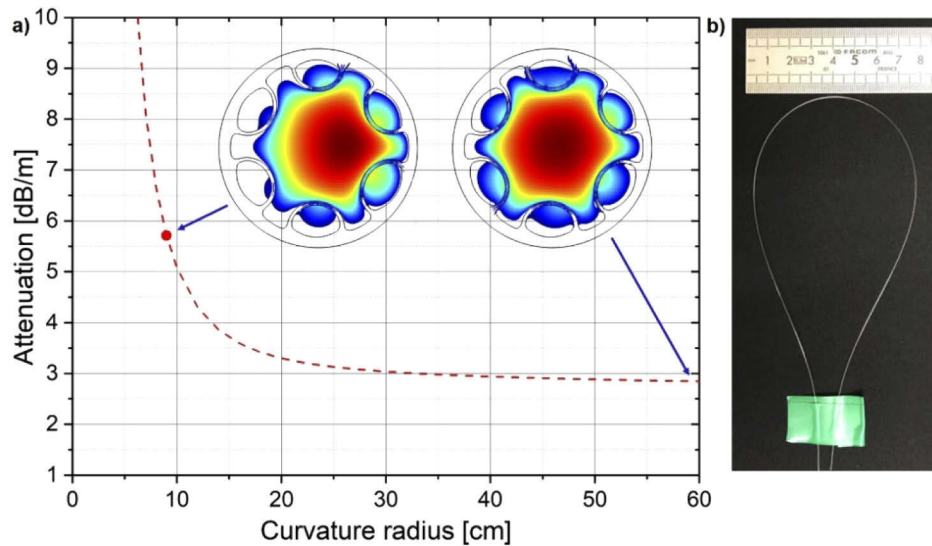


**Fig. 6.** (a) Bending loss simulation of Fiber B at 5.6  $\mu\text{m}$  wavelength. The insets show the fundamental mode at 5.6  $\mu\text{m}$ , for a fiber with a curvature radius of 60 cm and for a fiber with a curvature radius of 9 cm. (b) Demonstration of the flexibility of the fabricated tellurite HC-ARF coated with FEP polymer.

The critical bending radius, defined as the radius at which the loss becomes double that of the straight fiber is estimated to be 9 cm. Up to bend radii of about 20 cm the loss does not increase significantly. The inset of Fig. 6(b) shows the flexibility of the tellurite HC-ARF. The fiber can be bent with a curvature radius of 4 cm without breaking due to the extra mechanical strength provided by the FEP polymer coating.

To assess the modal quality of Fiber B, the  $M^2$  factor [25] was also measured at 5.6  $\mu\text{m}$  at the output of a 13 cm long fiber. In particular, the beam diameter was measured at different beam



positions by using a NanoScan 2s Pyro/9/5 pyroelectric detector. Figure 7 shows that an  $M^2$  of 1.2 was obtained, indicating that the HC-ARF supports nearly single mode behavior even after such a short length. We expect that an even lower  $M^2$  should be obtainable after longer lengths of fiber, due to the high differential loss of its high order modes.

To put this result into context, the HC-ARFs developed by Shiryayev et al. [9] and Gattass et al. [10] have transmission losses of the order of 3 dB/m at 4.8  $\mu\text{m}$  and 1.7 dB/m at 4.7  $\mu\text{m}$ , respectively. These values of loss are lower than the minimum loss of Fiber B. We believe that the good beam quality and the presence of a protective polymer coating, which give flexibility and protection to the fabricated fibers, represent the advantages of this work compared to these and other earlier attempts [8–10,12]. Furthermore, our simulations indicate that an improvement in the fabricated structure could result in loss smaller than 0.1 dB/m in the Mid-IR.

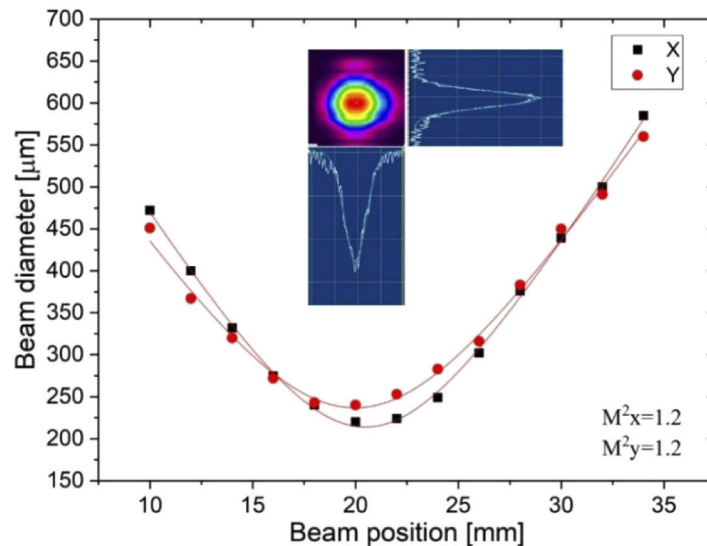


**Fig. 7.** Beam quality at the output of the tellurite antiresonant hollow core Fiber B at 5.6  $\mu\text{m}$  wavelength.

## 5. Understanding the effect of membrane thickness uniformity and shape

Since the fabricated tellurite HC-ARFs have some non-uniformities in the capillaries that affect both the shape and the non-equal thicknesses along their membranes, a modelling study was performed to assess the level of transmission loss that might be achieved by improving the fiber structure. In particular, Fiber B was investigated in more detail. An idealized structure of the fabricated fiber was designed (inset of Fig. 8 with blue contour), in which each of the 6 capillaries were kept the same size but their thickness was made uniform. We achieved this by drawing them as concentric circles, as shown in Fig. 8. The thickness of these circles is equal to the average radial thickness of each capillary. Simulating this structure indicates that by simply making the membranes more uniform in thickness, the loss would decrease to between 0.38 and 1 dB/m in the 5.5–6.2  $\mu\text{m}$  spectral range (dashed-dotted blue curve in Fig. 8).

To decrease the leakage loss further, the ID of the capillaries should be increased in order to push the outer solid cladding further away from the optical mode. To check how much lower the loss might go, an HC-ARF with circular capillaries was simulated (solid green curve). This fiber structure has the same core diameter and capillaries thickness as the idealized fiber structure. As can be seen, this reduced the loss by a further factor of 3 to 5. A loss lower than 0.4 dB/m can be

obtained between 5.35 and 6.15  $\mu\text{m}$ , with a minimum of 0.09 dB/m at 5.75  $\mu\text{m}$ . Despite the fact that the glass becomes pretty opaque after 6.1  $\mu\text{m}$ , see Fig. 2(b), modelling results show that an optical loss of 2 dB/m could be in principle obtained in an optimized tellurite HC-ARF at 6.5  $\mu\text{m}$ , nearly 5,000x lower than the glass absorption at that wavelength. This is due to the low overlap of the propagating fundamental mode with the cladding glass. To shift the operational window of the fabricated fiber to other wavelengths of operation, a different capillary thickness should be used. For example, to target the delivery of a CO laser at 5.4  $\mu\text{m}$ , the capillary thickness should be reduced from 5 to 4.4  $\mu\text{m}$ . In this way, the transmission band of the fiber would shift and produce a theoretical loss of 0.05 dB/m at 5.4  $\mu\text{m}$  (brown dotted curve of Fig. 8).

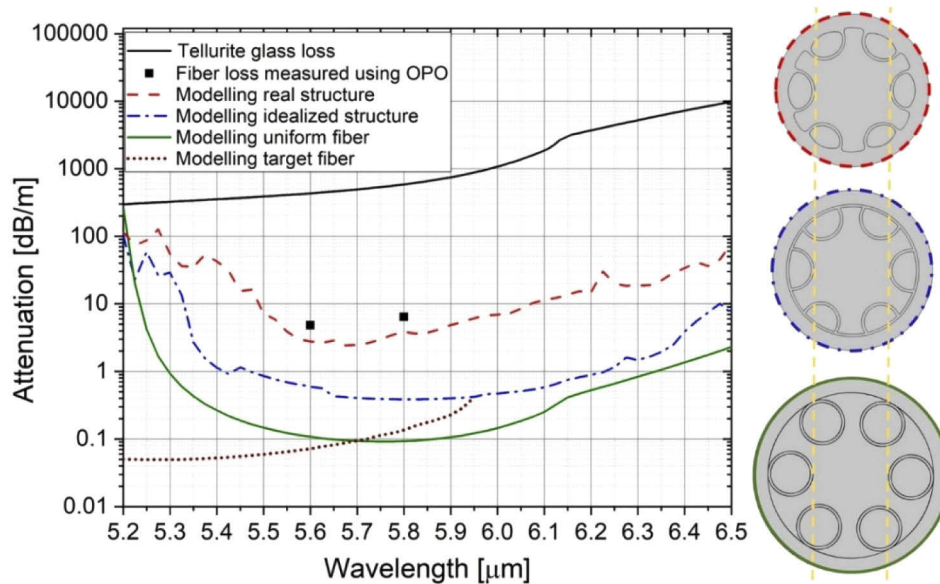


**Fig. 8.** Comparison between the experimental loss of Fiber B (black squared dots), the simulation of the real fiber structure (dashed red curve), the idealized fiber structure (dashed-dotted blue curve) and the optimized fiber structure (green solid curve). The brown dotted curve represents the simulated loss of the target fiber structure. The black solid curve represents the loss of the fabricated tellurite glass.

## 6. Conclusions

Flexible tellurite HC-ARFs coated with FEP polymer have been developed by an extrusion and draw approach. The use of extrusion allowed us to obtain a preform already consolidated with six fairly regularly arranged capillaries, which were then sleeved into a glass and polymer over-jacket and drawn to fibers. Thanks to the FEP polymer coating, the fibers can be coiled to radii down to 4 cm without permanent damage. Fiber losses of  $4.8 \pm 0.4$  and  $6.4 \pm 0.4$  dB/m were measured by using an OPO at 5.6 and 5.8  $\mu\text{m}$ , respectively. A good beam quality with an  $M^2$  of 1.2 was measured. A modelling study suggests that in order to decrease the loss further, more uniform thickness within each membrane should be targeted, with more circularly shaped capillaries also helping. A transmission loss lower than 0.3 dB/m between 5.4 and 6.1  $\mu\text{m}$  wavelength seems realistically possible. We thus believe that by improving the flow in the extrusion die to make the membranes more uniform and by applying more pressure into the capillaries to reduce the gaps and make them more circular, fibers with more uniform and circular capillaries can be obtained, opening up the possibility of flexible and long term durable fibers with sub 1-2 dB/m loss anywhere in the technologically important spectral region between 4.5 and 6.5  $\mu\text{m}$ .

## Funding

European Research Council (682724); Engineering and Physical Sciences Research Council (EP/P030181/1); Royal Society (NF170629); Ministerstvo Školství, Mládeže a Tělovýchovy (LM2015082); Engineering and Physical Sciences Research Council (EP/N00762X/1).

## Acknowledgments

All the data supporting this study are available from the University of Southampton repository at <https://doi.org/10.5258/SOTON/D1255>. This project gratefully acknowledges funding from the European Research Council (ERC), the EPSRC Airguide Photonics, the National Hub in High Value Photonics Manufacturing and the Royal Society. Juliano Hayashi thanks the Royal Society for the funding through the Newton International Fellowship. P. Janicek appreciates the financial support from the Ministry of Education, Youth and Sports of the Czech Republic.

## Disclosures

The authors declare no conflicts of interest.

## References

1. V. S. Aleinikov, V. P. Belyaev, N. D. Devyatkov, L. D. Mamedly, V. I. Masychev, and V. K. Sysoev, "CO laser applications in surgery," *Opt. Laser Technol.* **16**(5), 265–266 (1984).
2. J. S. Sanghera, L. B. Shaw, L. E. Busse, V. Q. Nguyen, P. C. Pureza, B. C. Cole, B. B. Harbison, I. D. Aggarwal, R. Mossadegh, F. Kung, D. Talley, D. Roselle, and R. Miklos, "Development and Infrared Applications of Chalcogenide Glass Optical Fibers," *Fiber Integr. Opt.* **19**(3), 251–274 (2000).
3. T. Arai and M. Kikuchi, "Carbon monoxide laser power delivery with an As<sub>2</sub>S<sub>3</sub> infrared glass fiber," *Appl. Opt.* **23**(17), 3017–3019 (1984).
4. J. S. Sanghera, C. M. Florea, L. B. Shaw, P. Pureza, V. Q. Nguyen, M. Bashkansky, Z. Dutton, and I. D. Aggarwal, "Non-linear properties of chalcogenide glasses and fibers," *J. Non-Cryst. Solids* **354**(2-9), 462–467 (2008).
5. F. Poletti, "Nested antiresonant nodeless hollow core fiber," *Opt. Express* **22**(20), 23807 (2014).
6. A. N. Kolyadin, A. F. Kosolapov, A. D. Pryamikov, A. S. Biriukov, V. G. Plotnichenko, and E. M. Dianov, "Light transmission in negative curvature hollow core fiber in extremely high material loss region," *Opt. Express* **21**(8), 9514–9519 (2013).
7. F. Yu and J. C. Knight, "Spectral attenuation limits of silica hollow core negative curvature fiber," *Opt. Express* **21**(18), 21466 (2013).
8. A. F. Kosolapov, A. D. Pryamikov, A. S. Biriukov, V. S. Shiryayev, M. S. Astapovich, G. E. Snopatin, V. G. Plotnichenko, M. F. Churbanov, and E. M. Dianov, "Demonstration of CO<sub>2</sub>-laser power delivery through chalcogenide-glass fiber with negative curvature hollow core," *Opt. Express* **19**(25), 25723–25728 (2011).
9. V. S. Shiryayev, A. F. Kosolapov, A. D. Pryamikov, G. E. Snopatin, M. F. Churbanov, A. S. Biriukov, T. V. Kotereva, S. V. Mishinov, G. K. Alagashev, and A. N. Kolyadin, "Development of technique for preparation of As<sub>2</sub>S<sub>3</sub> glass preform for hollow core microstructured optical fibers," *J. Optoelectron. Adv. Mater.* **16**(9–10), 1020–1025 (2014).
10. R. R. Gattass, D. Rhonehouse, D. Gibson, C. C. McClain, R. Thapa, V. Q. Nguyen, S. S. Bayya, R. J. Weiblen, C. R. Menyuk, L. B. Shaw, and J. S. Sanghera, "Infrared glass-based negative-curvature antiresonant fibers fabricated through extrusion," *Opt. Express* **24**(22), 25697–25703 (2016).
11. W. Belardi and P. J. Sazio, "Borosilicate Based Hollow-Core Optical Fibers," *Fibers* **7**(8), 73 (2019).
12. H. T. Tong, N. Nishiharaguchi, T. Suzuki, and Y. Ohishi, "Mid-infrared transmission by a tellurite hollow core optical fiber," *Opt. Express* **27**(21), 30576 (2019).
13. B. Zhou, C. F. Rapp, J. K. Driver, M. J. Myers, J. D. Myers, J. Goldstein, R. Utano, and S. Gupta, "Development of tellurium oxide and lead-bismuth oxide glasses for mid-wave infra-red transmission optics," *Proc. SPIE* **8626**, 86261F (2013).
14. V. D. Fedorov, V. V. Sakharov, A. M. Provorova, P. B. Baskov, M. F. Churbanov, V. S. Shiryayev, M. Poulain, M. Poulain, and A. Boutarfaia, "Kinetics of isothermal crystallization of fluoride glasses," *J. Non-Cryst. Solids* **284**(1-3), 79–84 (2001).
15. J. Bei, H. T. Cheung Foo, G. Qian, T. M. Monro, A. Hemming, and H. Ebendorff-Heidepriem, "Experimental study of chemical durability of fluorozirconate and fluorindate glasses in deionized water," *Opt. Mater. Express* **4**(6), 1213–1226 (2014).
16. O. Mouawad, C. Strutynski, J. Picot-Clément, F. Désévéday, G. Garnet, J.-C. Jules, and F. Smektala, "Optical aging behavior naturally induced on As<sub>2</sub>S<sub>3</sub> microstructured optical fibers," *Opt. Mater. Express* **4**(10), 2190–2203 (2014).
17. G. Tao, H. Ebendorff-Heidepriem, A. M. Stolyarov, S. Danto, J. V. Badding, Y. Fink, J. Ballato, and A. F. Abouraddy, "Infrared fibers," *Adv. Opt. Photonics* **7**(2), 379–458 (2015).

18. Heraeus, "Transmission Calculator" [http://www.heraeus.com/en/hca/fused\\_silica\\_quartz\\_knowledge\\_base\\_1/t\\_calc\\_1/transmission\\_calculator\\_hca.html](http://www.heraeus.com/en/hca/fused_silica_quartz_knowledge_base_1/t_calc_1/transmission_calculator_hca.html).
19. Du Pont, "FEP handbook" [http://www.rjchase.com/fep\\_handbook.pdf](http://www.rjchase.com/fep_handbook.pdf).
20. Fluorotherm, "FEP Properties" <https://www.fluorotherm.com/technical-information/materials-overview/fep-properties/>.
21. Q. Fu, L. Xu, P. C. Shardlow, D. P. Shepherd, S.-U. Alam, and D. J. Richardson, "High-beam-quality, watt-level, widely tunable, mid-infrared OP-GaAs optical parametric oscillator," *Opt. Lett.* **44**(11), 2744–2747 (2019).
22. J. P. Berenger, "A Perfectly Matched Layer for the Absorption of the Electromagnetic Waves," *J. Comput. Phys.* **114**(2), 185–200 (1994).
23. I. A. Bufetov, A. F. Kosolapov, A. D. Pryamikov, A. V. Gladyshev, A. N. Kolyadin, A. A. Krylov, Y. P. Yatsenko, and A. S. Biriukov, "Revolver Hollow Core Optical Fibers," *Fibers* **6**(2), 39 (2018).
24. M. Heiblum and J. H. Harris, "Analysis of Curved Optical Waveguides by Conformal Transformation," *IEEE J. Quantum Electronics* **11**(2), 75–83 (1975).
25. A. E. Siegman, "New developments in laser resonators," *Proc. SPIE* **1224**, 2 (1990).